Scientific Research Publishing

New Journal of Glass and Ceramics, 2023, 13, 1-16
https://www.scirp.org/journal/njgc
ISSN Online: 2161-7562
ISSN Print: 2161-7554

Chemical Durability, Properties and Structural Approach of the Glass Series xFe_2O_3-(45-x) PbO-$55P_2O_5$ (with $0 \leq x \leq 20$; mol%)

Radouane Makhlouk[1], Zineb Chabbou[1], Yassine Er-rouissi[1], M'hammed Taibi[2], Said Aqdim[1,3*]

[1]Laboratory of Materials Engineering for Environment and Valorization, Faculty of Sciences, Hassan II University Ain Chock, Casablanca, Morocco
[2]Physico-Chemistry Laboratory of Inorganic and Organic Materials ENS, University Md V, Rabat, Morocco
[3]Mineral Chemistry, Department of Chemistry, Faculty of Science, Hassan II University Ain Chock, Casablanca, Morocco
Email: *said_aq@yahoo.fr

How to cite this paper: Makhlouk, R., Chabbou, Z., Er-rouissi, Y., Taibi, M. and Aqdim, S. (2023) Chemical Durability, Properties and Structural Approach of the Glass Series xFe_2O_3-(45-x) PbO-$55P_2O_5$ (with $0 \leq x \leq 20$; mol%). *New Journal of Glass and Ceramics*, **13**, 1-16.
https://doi.org/10.4236/njgc.2023.131001

Received: November 22, 2022
Accepted: January 27, 2023
Published: January 30, 2023

Abstract

The synthesis for glasses series xFe_2O_3-(45-x)PbO-$55P_2O_5$, (with $0 \leq x \leq 20$; mol%) carried out in a temperature (1050 ± 10)˚C, leads to obtaining transparent glasses, brown in color and with a non-hygroscopic appearance. The study of glasses dissolution rate, immersed in distilled water at 90˚C for 24 days, indicates a considerable chemical durability. The increase in the Fe_2O_3 content in the vitreous network to the detriment of PbO is a favorable factor for the chemical durability improvement. Different techniques have been used such as X-ray diffraction, infrared spectroscopy, DSC, SEM and density for the study of these glasses. These techniques have led to establish correlations between chemical and structural properties. Thus the results obtained confirmed the creation of P-O-M bonds (M = Pb, Fe) with a strongly covalent nature to the detriment of the hydrated P-O-P bonds and led to the formation, mainly, of pyrophosphate groups. The low melting point of Pb-O makes it possible to play an important role, at the same time, on the viscosity, on the equilibrium between the vitreous bath and the crystallites formed. The dissolution rate obtained is 100 times smaller than that of silicate glasses used as an alternative form for the vitrification of radioactive waste.

Keywords

Phosphate Glasses, Lead, Iron, Density, IR, DRX, MEB, Durabilité Chimique, Vitrification, Nuclear Wastes

1. Introduction

Phosphate glasses have been investigated principally because of their relatively

low processing temperatures (1000˚C - 1100˚C) compared with borosilicate glasses (1200˚C - 1500˚C). Their properties, such as a low melting point, high coefficient of thermal expansion, dielectric properties and optical properties, make these glasses potential candidates for many technological applications such as: medical field (biomaterials), solid electrolytes, vitrification of nuclear waste, etc. [1]-[11]. Recently, the glass structure in the $PbO\text{-}P_2O_5$ binary system has been studied. Moreover, the incorporation of Pb-O into the phosphate network would have resulted in the breaking of hydrated P-O-P bonds and the appearance of covalent and rigid P-O-Pb bands [10]. In the previous work we are confirmed that the substitution of Na_2O with lead oxide by more than 28 mol%, with the presence of 2 mol% of Cr_2O_3 in the vitreous network appeared to be an unfavourable factor for chemical durability. The phenomenon has been explained by the approach of the boundary zone between the crystal and the glass by the continuous formation of isolated phosphate groups PO_3^{4-} [7] [12] [13]. Hence, the crystallites exceed a certain limit, and the equilibrium between the glass bath and these crystallites is no longer maintained; we notice, once, a few decrease in the chemical durability. The aim of the present work is to study the mixed effects of lead and iron on the structure and to improve the chemical durability by reducing the PbO rate by substitution with Fe_2O_3 content which will lead to the decrease of isolated orthophosphate groups by promoting the formation of pyrophosphate groups [7], and consequently the decrease in the crystallites number which prevents the equilibrium formation between these and the vitreous bath. The study of the dissolution rate as a function of iron oxide content in distilled water at 90˚C for the glass series $xFe_2O_3\text{-}(45\text{-}x)PbO\text{-}55P_2O_5$ with ($0 \le x \le 20$; mol%) reveals an important chemical durability. The relatively low melting point of Pb-O makes it possible to play an important role, at the same time, on the viscosity and on the equilibrium between the vitreous bath and the crystallites formed. The dissolution rate (D_R) of the analyzed compounds is 100 times less than the values of borosilicate glasses and 200 times less than BaBal glass which is used as alternative material for the immobilization of nuclear waste substances.

2. Experimental Section

The synthesis of phosphate-based glasses was carried out by direct fusion of mixed reagents $(NH_4)_2HPO_4$, $Pb(NO_3)_2$ and Fe_2O_3 in adequate proportions. The reagents were finely ground and then introduced into a porcelain crucible. They were first heated at 300˚C for 1 hour and then at 500˚C for 1 hour to complete their decomposition. The mixture reaction was then heated to (1050 ± 10)˚C for 20 min. The liquid obtained is homogeneous. It was then poured into an aluminum plate previously heated to 200˚C to avoid thermal shocks. The chemical durability of these glasses was evaluated by the weight loss of the sample. The samples were then polished with carbon silica sandpaper (CSI), cleaned with acetone and immersed in Pyrex beakers containing 100 ml of distilled water and

brought to 90˚C. The surface of the sample must be constantly immersed in distilled water for 24 days. The glass density was measured at room temperature using Archimedes' method. The glass was immersed in a solution of diethyl orthophtalate whose density, depending on the temperature, was known. The precision is 0.05 g/cm^3. The infrared spectra of the studied phosphate glasses were located in the region between 400 and 1600 cm^{-1} with a resolution of 2 cm^{-1}. The samples were finely ground and mixed with KBr (potassium bromide), which was transparent in the infrared, and whose role was to serve as a matrix. The microstructures of the sample glasses were characterized by scanning electron microscopy (SEM), equipped with a full system micro-analyser (EDX-EDAX).

3. Results and Discussion

3.1. Location of the Studied Glasses in the Fe_2O_3-PbO-P_2O_5 Ternary Diagram

As can be seen clearly from the ternary diagram (Figure 1) and taking into account the oxygen/phosphate ratios shown in Table 1. The location of S_0, S_5, S_{10}, S_{15} and S_{20} indicated that the structure of meta-phosphate chains (S_0 and S_5) evolved to predominant short pyrophosphate groups (S_{15} to S_{20}).

3.2. Chemical Durability Analysis and pH of Glasses of the xFe_2O_3-(45-x)PbO-$55P_2O_5$ System (with ($0 \le x \le 20$ mol%)

The chemical durability of the studied glasses series was approached using the measurement of the dissolution rate, which was defined as the weight loss of the glass expressed in g·cm^{-2}·min^{-1}. The values of the dissolution rate (D_R), as a function of the Fe_2O_3 molar percentage, are grouped in Table 1 and presented in

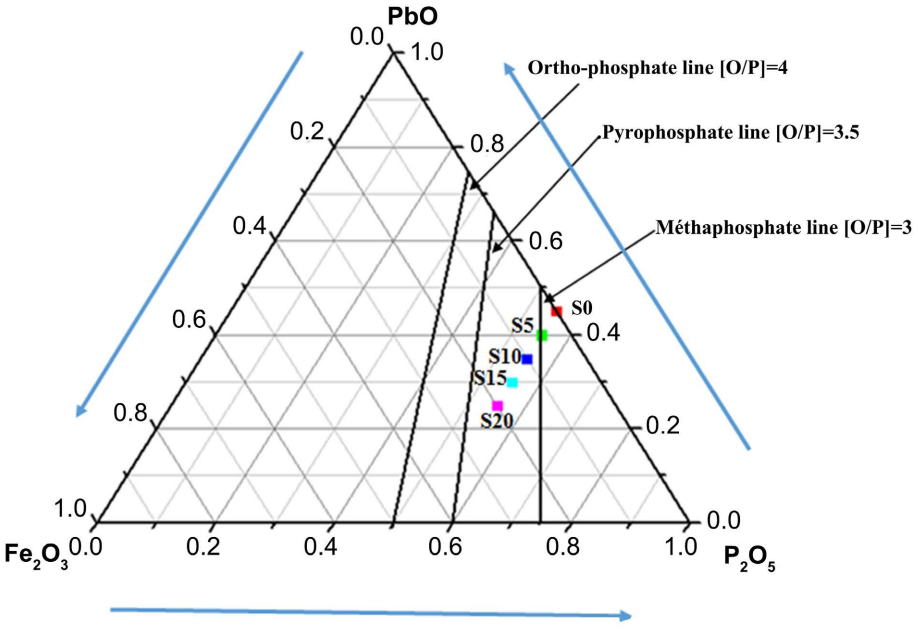

Figure 1. Localization in the ternary diagram, of system glasses xFe_2O_3-(45-x)PbO-$55P_2O_5$ (avec $0 \le x \le 20$; mol%).

Table 1. Compositions, chemical durability and pH of the glass series xFe_2O_3-(45-x)PbO-$55P_2O_5$ system with ($0 \le x \le 20$ mol%)

Échantillon de verre	Composition de verre de départ (mol%)			O/P ratio	(D_R) ($g \cdot cm^{-2} \cdot min^{-1}$)	pH
	Fe_2O_3	PbO	P_2O_5		24 days	±0.5
S_0	0	45	55	**2.90**	$(3.4 \pm 0.2) \times 10^{-6}$	**5.2 ± 0.5**
S_5	5	40	55	**3**	$(5.6 \pm 0.2) \times 10^{-6}$	**5.1 ± 0.5**
S_{10}	10	35	55	**3.09**	$(9.9 \pm 0.2) \times 10^{-7}$	**6.2 ± 0.5**
S_{15}	15	30	55	**3.18**	$(1.5 \pm 0.2) \times 10^{-8}$	**6.5 ± 0.5**
S_{20}	20	25	55	**3.27**	$(2.9 \pm 0.2) \times 10^{-10}$	**7.2 ± 0.5**

Figure 2. The typical results obtained for the samples, after their immersion in 100 ml of distilled water and heated at 90˚C for 24 consecutive days, showed a remarkable chemical durability as the Fe_2O_3 content increased in the vitreous network to the detriment of PbO content. **Figure 3** shows the pH of the aqueous solution after the corrosion tests. Due to the high chemical durability of glasses containing more than 10 mole % Fe_2O_3 the pH decreases slightly from its initial values. However, there is a relatively significant decrease in the pH of solutions for immerged glasses with a less Fe_2O_3 content than 10 mol%. The decrease in pH between 5.2 and 7.2 is attributed to the formation of phosphoric acid whose pH generally, varies between 5 and 11, due to the degradation of glass by water, which plays an amphoteric role [14]. The decrease in pH is consistent with the large values of D_R. The visual appearance of glassy compounds emerged in distilled water at 90˚C for 24 days shows that glasses which have low Fe_2O_3 content such as S0 and S5 are relatively corroded, while S_{15} and S_{20} glasses are practically intact and keep their original appearance [15].

3.3. Analysis by Differential Scanning Calorimetry (DSC)

Figure 4 shows the DSC curves of iron-lead phosphate glasses. The results of the glass transition temperatures (T_g) as a function of the Fe_2O_3 content are grouped in **Table 2** and presented in **Figure 5**. The T_g evolution indicated that the substitution of lead oxide by iron oxide led to an almost linear increase in T_g. The analysis of these results indicated a significant improvement in T_g when the Fe_2O_3 content increased, this increase characterizes a strengthening of the vitreous networks [8] [14] [16] [17]. This behavior has been confirmed by previous work [14]. For the S_0 sample ($45PbO\text{-}55P_2O_5$) the two endothermic peaks around 70˚C and 193˚C are due to the dehydration of the sample while the endothermic peaks which appear in the interval 376 - 470˚C are tuned to the glass transition temperatures of different samples.

3.4. Density and Molar Volume of the Glass Series of Composition xFe_2O_3-(45-x) $PbO\text{-}55P_2O_5$ (with Avec ($0 \le x \le 20$; mol%)

The density measurements made it possible to follow the evolution of the molar

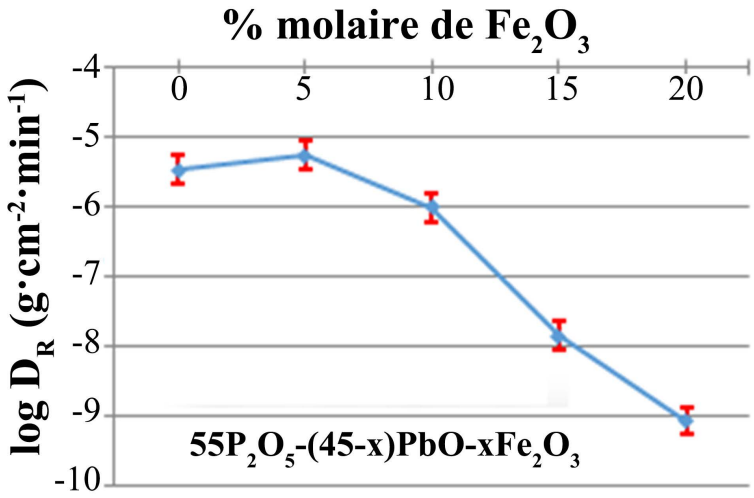

Figure 2. Chemical durability of the glass series $55P_2O_5$-(45-x)PbO-xFe_2O_3 (with ($0 \leq x \leq 20$ mol%) as a function Fe_2O_3 (mol%).

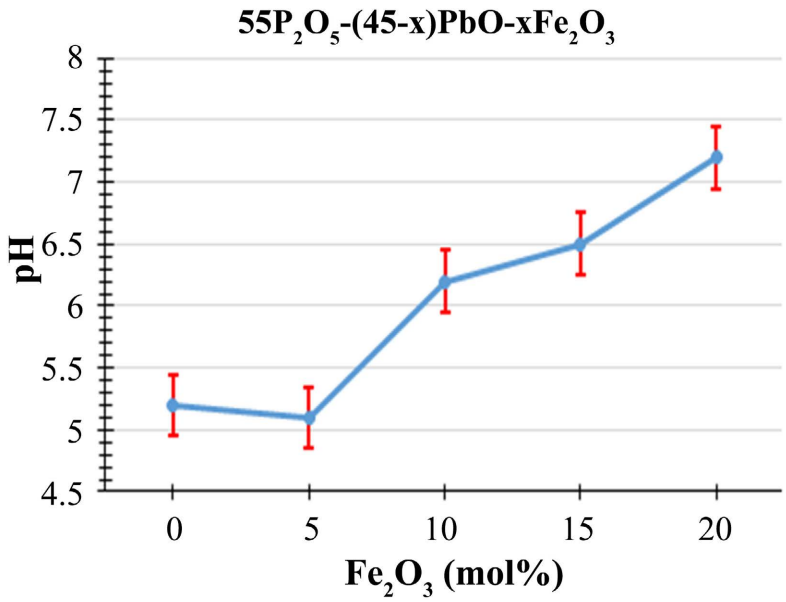

Figure 3. pH curve of phosphate glasses leaching, after 24 days of attack, as a function of Fe_2O_3 content (mol%).

Table 2. Compositions and transition temperature (T_g) of the glass series xFe_2O_3-(45-x)PbO-$55P_2O_5$ system with ($0 \leq x \leq 20$ mol%)

Sample	starting mixted oxide (mol%)			T_g (°C) (±2)
	Fe_2O_3	PbO	P_2O_5	
S_0	0	45	55	376
S_5	5	40	55	**415**
S_{10}	10	35	55	**432**
S_{15}	15	30	55	**470**
S_{20}	20	25	55	**501**

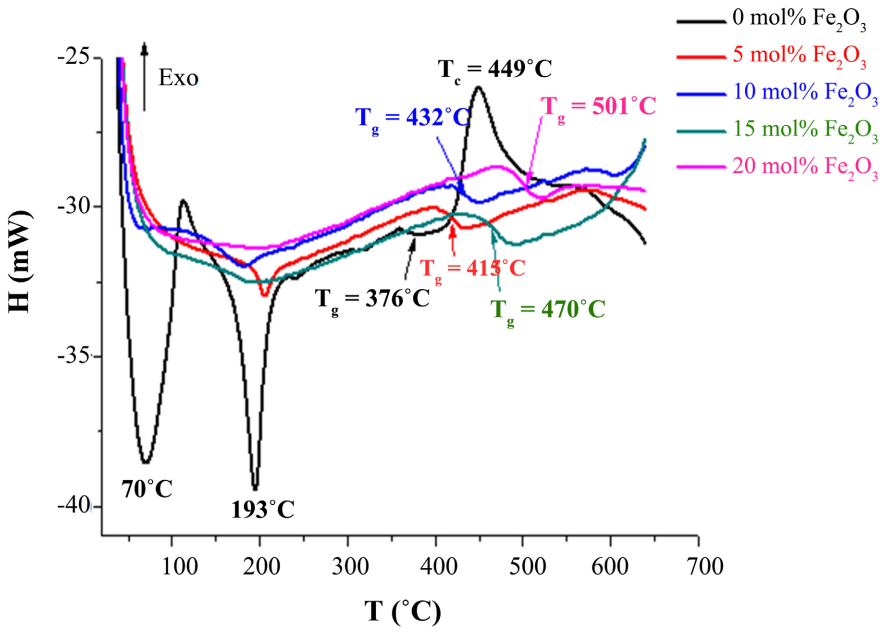

Figure 4. Thermogram curves of the composition phosphate glass series xFe_2O_3-(45-x) PbO-$55P_2O_5$.

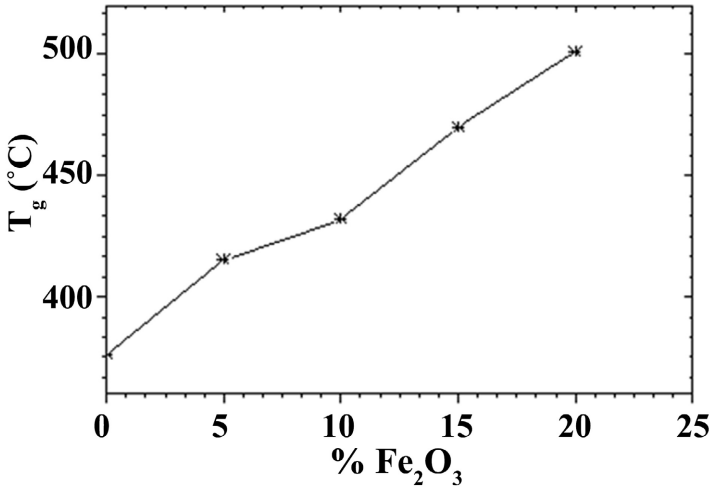

Figure 5. Variation of T_g versus Fe_2O_3 content for the glass series $55P_2O_5$-(45-x)PbO-xFe_2O_3 (with ($0 \le x \le 20$ mol%).

volume according to the composition of the glass along the xFe_2O_3-(45-x) PbO-$55P_2O_5$ system, which was measured at room temperature. As can be deduced from Table 3 and from the curve in Figure 6, we notice an increase in the density of the glass from 3.86 to 4.35 (g/cm^3) when the Fe_2O_3 content varies, respectively, from 0 to 20 mol%. This increase leads to reinforce the vitreous network bonds by replacing the hydrated P-O-P bonds by covalent and rigid Fe-O-P bonds. The glass density is given by the follow equation:

$$\rho = \frac{m_{\text{glass}}}{\left[m_{\text{glass}} + \left(m_{\text{ortho}} - m_{\text{ortho+glass}}\right)\right]} \rho_{\text{ortho}}$$

Table 3. Compositions, density and related molar data of the glass series xFe_2O_3-(45-x)PbO-$55P_2O_5$.

Molaire formula Nombre d'O/mol (N_0)	Molaire Mass (g/mol)	Density ρ, (g/cm³)	Molar Volume (nm)³ $V_{OM} = M/\rho N_A \cdot N_0$	Calculated oxygen Radius (nm) r_{cal} (O^{-2}) (nm)
$0Fe_2O_3$-45PbO-$55P_2O_5$ (320)	**17,854**	**(3.86 ± 0.02)**	**0.0240**	**0.144**
$5Fe_2O_3$-40PbO-$55P_2O_5$ (330)	**17,536**	**(3.87± 0.02)**	**0.0228**	**0.141**
$10Fe_2O_3$-35PbO-$55P_2O_5$ (340)	**17,218**	**(3.97± 0.02)**	**0.0211**	**0.138**
$15Fe_2O_3$-30PbO-$55P_2O_5$ (350)	**16,900**	**(4.12± 0.02)**	**0.0194**	**0.134**
$20Fe_2O_3$-25PbO-$55P_2O_5$ (360)	**16,582**	**(4.35± 0.02)**	**0.0175**	**0.129**

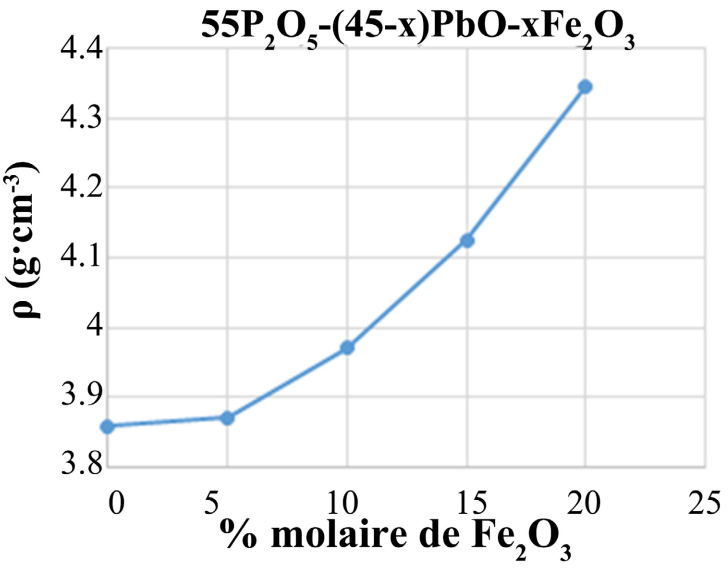

Figure 6. Variation of density versus Fe_2O_3 content for the glass series xFe_2O_3-(45-x)PbO-$55P_2O_5$ (with $0 \le x \le 20$; mol%).

with:

ρ = Density

m_{glass} = Weight of glass measured in air

m_{ortho} = Weight of diethyl orthophthalate only

$m_{ortho+glass}$ = Weight of glass immersed in diethyl orthophthalate

ρ_{ortho} = 1.11422 g/cm³

The molar volume (V_{OM}) and the oxygen anionic radius r_{cal} (O^{2-}) in the glass were determined from Equations (1) and (2), respectively:

$$V_{OM} = M/\rho N_A \cdot N_0 \quad (1)$$

$$r_{cal} = \sqrt[3]{V_{OM}}/2 \quad (2)$$

with M = molar mass.

ρ = density.

N_A = Avogadro's number.

N_0 = number of oxygen contained in the molar formula.

Data analysis in Table 4 showed that, both, the molar volume and the anionic radius value of relative oxygen r_{cal} (O^{2-}), calculated by Equation (2), decreased when the Fe_2O_3 content increased at the expense of PbO. [13] [16]. It should also be noted that the anionic radius of oxygen r_{cal} (O^{2-}) decreased when the composition of the glass tended to pass from ultra and meta-phosphate domains (S_0, S_5) (O/P = 2.9, 3) to pyrophosphate domain (S_{20}) (O/P = 3.27), such a decrease in r_{cal} (O^{2-}) highlights a strengthening of the Fe-O-P bond in the vitreous network which is interpreted by a shortening of the interatomic distances due to the purely covalent character coordination bonds [14] [17] [18].

3.5. Infrared Spectroscopy (IR) of the Glass Series xFe_2O_3-(45-x)PbO-$55P_2O_5$ with ($0 \le x \le 20$; mol%)

The infrared spectra of the glass series xFe_2O_3-(45-x) PbO-$55P_2O_5$ are shown in Figure 7. All phosphate vibration bands of the treated samples were situated in the frequency domain between 1600 - 399 cm^{-1} [17] [18]. The band between 466 - 500 cm^{-1} was attributed to the δ (P-O-P) skeleton vibration mode [17] [18]. We also noted that the 1210 - 1228 cm^{-1} band attributed to the ν_{as} (PO_2) vibration mode of the meta-phosphate groups (Q^2) becomes a simple shoulder when the molar content of Fe_2O_3 reached 20 mol%, while the band located between 1000 - 1060 cm^{-1} moved towards high frequencies giving a wide band attributed to the vibration mode ν_{as} (PO_3) of pyrophosphate groups (Q^1) [19] [20]. The band observed at 1000 cm^{-1}, when x = 0, can be attributed to the isolated orthophosphate group PO_4^{3-} (Q^0) [19]. The band located at 755 - 766 cm^{-1}, attributed to the ν_s (P-O-P) vibration mode, moved towards high frequencies when the Fe_2O_3 oxide content increased and indicated the formation of non-bridge oxygens of the di-phosphate groups (Q^1) to the detriment of the meta-phosphate groups (Q^2).

3.6. X-ray Diffraction of the Glasses Composition xFe_2O_3-(45-x)PbO-$55P_2O_5$ with ($0 \le x \le 20$; mol%)

To study the amorphous state of the prepared glasses, X-ray diffraction analyses were carried out on all the prepared samples. The results obtained in Figure 8,

Table 4. Variation of the ratio [FeII]/[FeII + FeIII] versus mol% Fe_2O_3 along the glass series xFe_2O_3-(45-x)PbO-$55P_2O_5$.

Composition (mole %)	Rapport Fe^{2+}/Fe_T, % (±2)	Fe_2O_3 (mole %)
Fe_2O_3-40PbO-$55P_2O_5$	**26**	**5**
$10Fe_2O_3$-35PbO-$55P_2O_5$	**21.57**	**10**
$15Fe_2O_3$-30PbO-$55P_2O_5$	**7.02**	**15**
$20Fe_2O_3$-25PbO-$55P_2O_5$	**6.67**	**20**

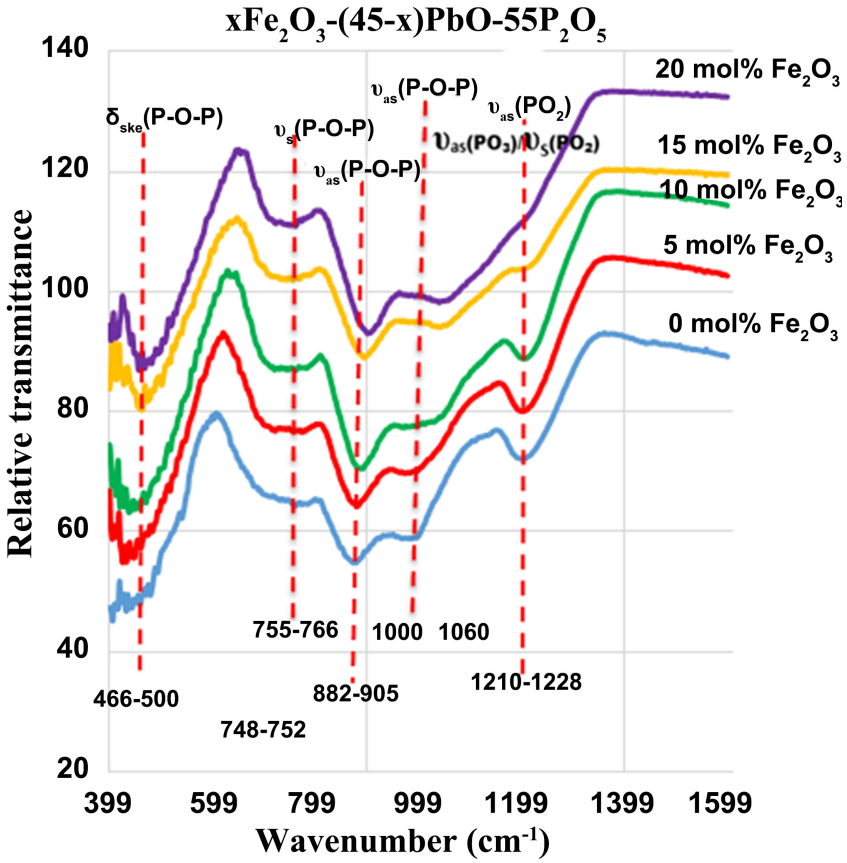

Figure 7. IR spectra of phosphate glass series xFe_2O_3-(45-x)PbO-$55P_2O_5$, with ($0 \le x \le 20$; mol%).

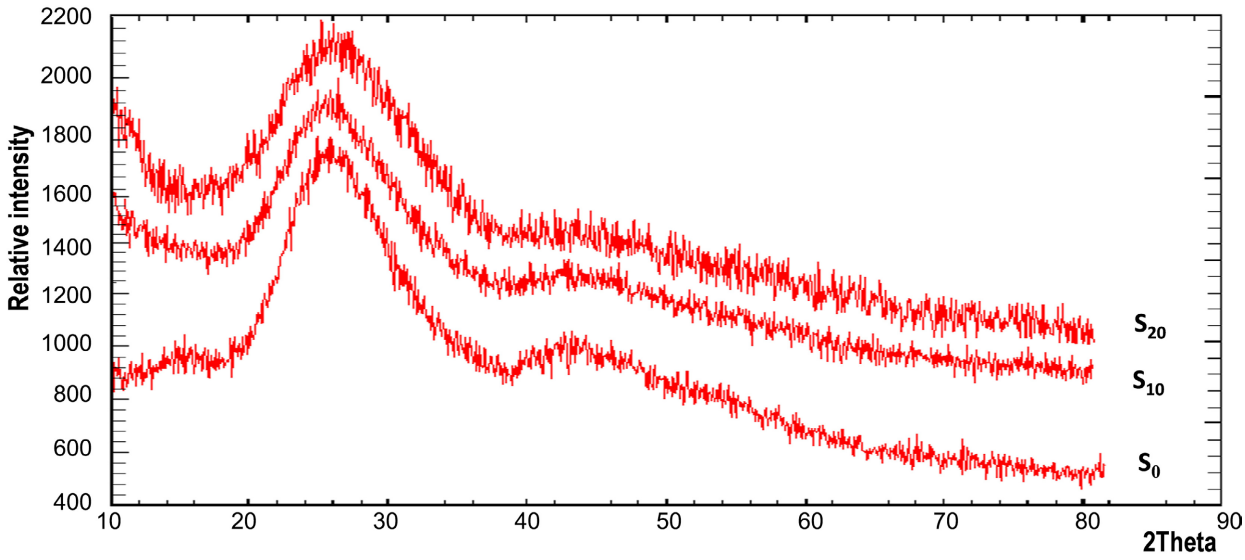

Figure 8. X-ray diffraction of the S_0, S_{10} et S_{20} samples phosphate glasses.

confirmed the amorphous character which reflects a disordered structure. As expected, the analysis by X-ray diffraction of annealed glasses S_0, S_{10} and S_{20} respectively, at 580˚C and 620˚C for 72 hours, are presented in Figure 9. The analysis

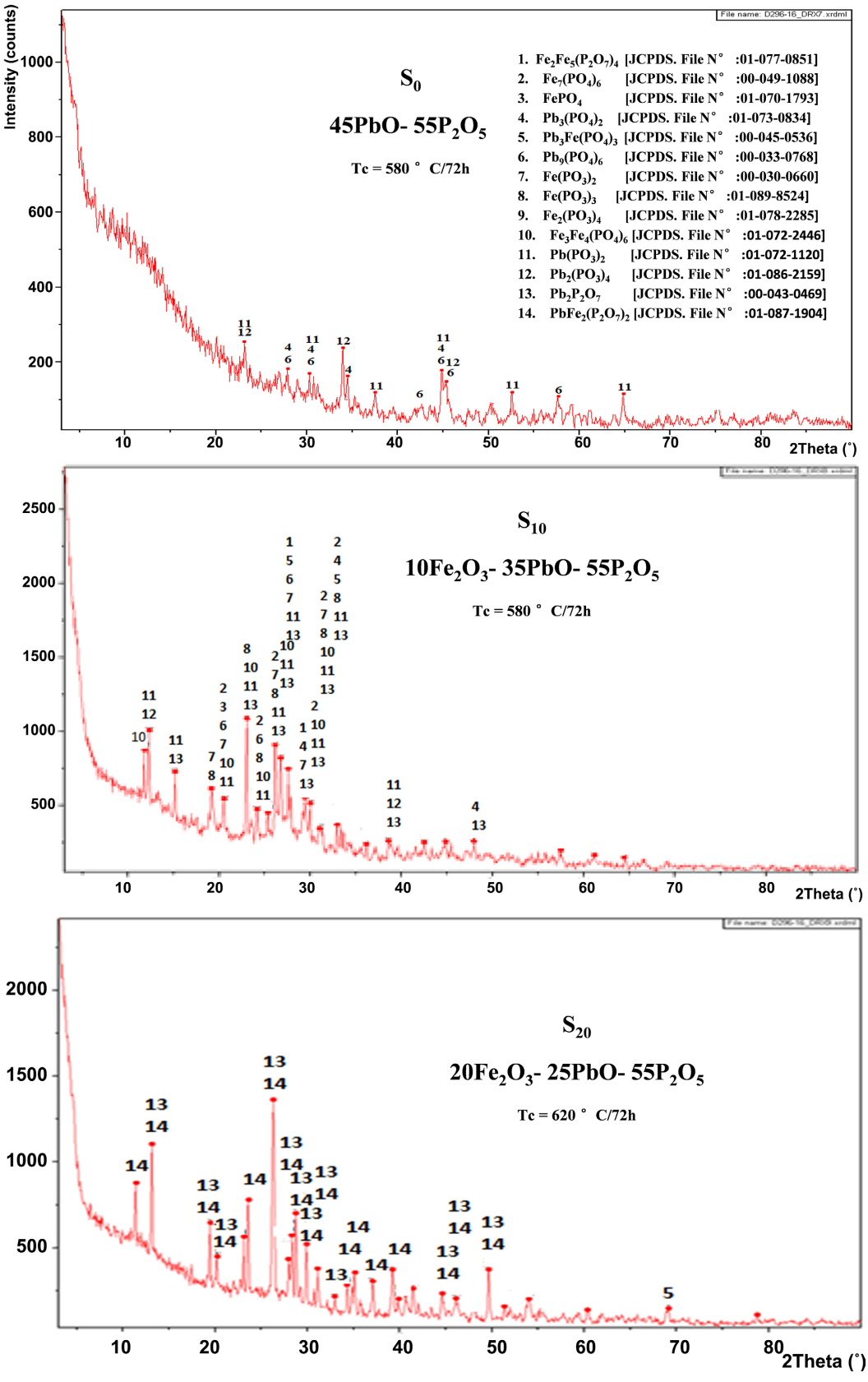

Figure 9. X-ray diffraction of S_0, S_{10} et S_{20} samples anneled glasses, respectivement at 580˚C and 620˚C pendant 72 h.

of these spectra indicated the appearance of peaks mixture linked to meta-phosphate, ortho-phosphate and pyrophosphate phases. On the other hand, it indicated a radical change in the structure, when the iron oxide content increased in the vitreous network, showing that the studied glasses structure evolved from the meta-phosphate (presumably cyclic) and the isolated ortho-phosphate phases to majorities pyrophosphate phases while we moved from S_0, S_{10} to S_{20}. The x-ray diffraction spectra obtained from the S_{10} sample tended to crystallize as a mixture of meta-phosphate, ortho-phosphates and pyrophosphates with majorities of meta-phosphate and/or rings meta-phosphate phases. However, in the S_{20} sample, we noticed that the meta-phosphate phases disappeared and the main phases called pyrophosphates such as $PbFe_2(P_2O_7)_2$ and $Pb_2P_2O_7$ were mostly intense in the sample [21] [22].

3.7. Scanning Electron Microscopy (SEM) Analysis of Glass Series xFe_2O_3-(45-x)PbO-$55P_2O_5$ with ($0 \le x \le 20$; mol%)

The scanning electron microscopy (SEM) micrographs presented in **Figure 10** illustrated the morphology of the studied glasses. The micrographs of **Figures 10(a)-(c)** showed the existence of two phases, a vitreous phase and a crystalline phase. It also indicated the formation of agglomerates in the crystalline phase of different sizes, ranging from a few microns to several tens of microns, as shown by the different images attributed respectively to samples S_0, S_{10} and S_{20} [7] [17] [19] [21]. A deep of SEM micrograph analysis of the glasses considered in this work indicated the glass form of S_0 shown in **Figure 10(a)**, exhibited the presence of an overload crystalline phases with different form and size [12] [23] [24]

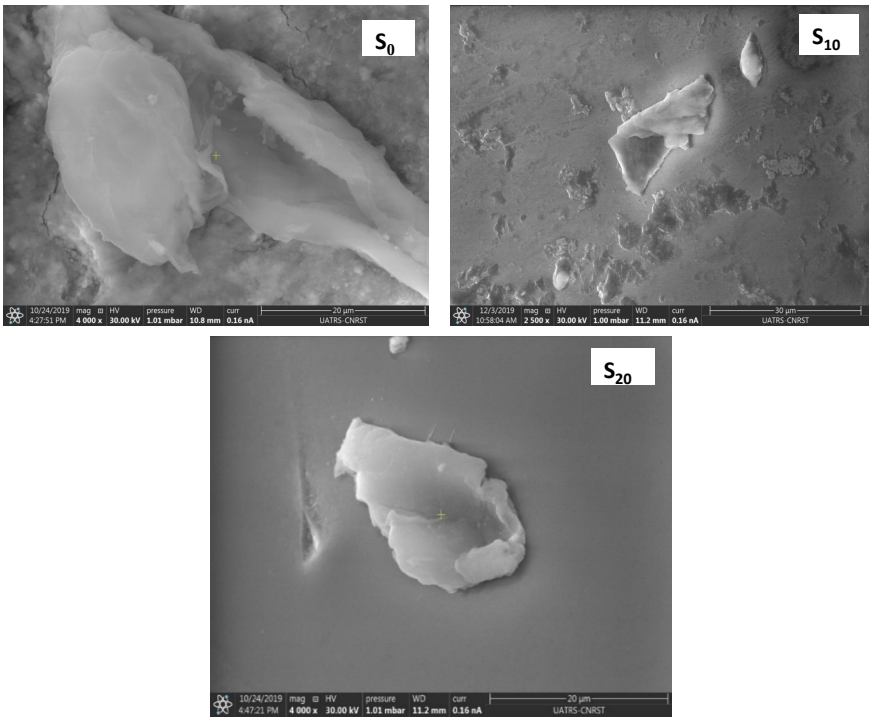

Figure 10. Scanning electronic micrograph of S_0, S_{10} and S_{20} samples phosphate glasses.

[25]. When the Fe_2O_3 content increased in the glass, the number of crystallites decreased as seen in the S_{10} (**Figure 10(b)**) and S_{20} (**Figure 10(c)**) samples, respectively. Hence, SEM analysis confirmed a relatively large homogenous vitreous phase with the coexistence of crystalline particles in the S_{20} sample which has the maximum Fe_2O_3 content. Some different crystalline phases were identified by XRD and it seems that a decrease of crystallization tendency was enhanced and $PbFe_2(P_2O_7)_2$, $Pb_2P_2O_7$, phases were crystallized in the last sample (S20) with some traces of $Pb_3Fe(PO_4)_3$ phases. This explains that the structure changes towards more short pyrophosphates at the detriment of metaphosphates and shorter isolated orthophosphate chains as the Fe_2O_3 content increases in the glass network [17] [19] [21] [26] [27].

3.8. Iron(II)/Iron(III) Redox Phenomenon

Like all transition elements, iron was reputed to have at least two oxidation degrees under normal atmospheric conditions. Therefore, as expected the starting iron(III) oxide has been reduced during the elaboration of the title phosphate glasses. Indeed the batch melting is realized in a rather reduced atmosphere which is created by the decomposition of the starting compound $(NH_4)_2HPO_4$ which gives rise at high temperatures, to a gas mixture of the type $(NH_{3(}g) + H_2 + H_2O(g))$ [16] [17] [22] [28]. Analysis of the results (**Figure 11**) shows that all the glasses studied underwent a reduction at the time of melting, from the Fe(III) state to the Fe(II) state. The study of this reduction shows that it decreases when the Fe_2O_3 content exceeds 10 mol%. This reduction does not exceed, in general under normal atmospheric conditions, 10%. However, in the case of iron-lead-phosphate glasses, the reduced Fe(III) rate reaches higher values for low iron oxide content, this can be explained by the oxidation in atmospheric air of a part of PbO into PbO_2 leading to a greater reduction of Fe(III) to Fe(II) [7] [14] [17].

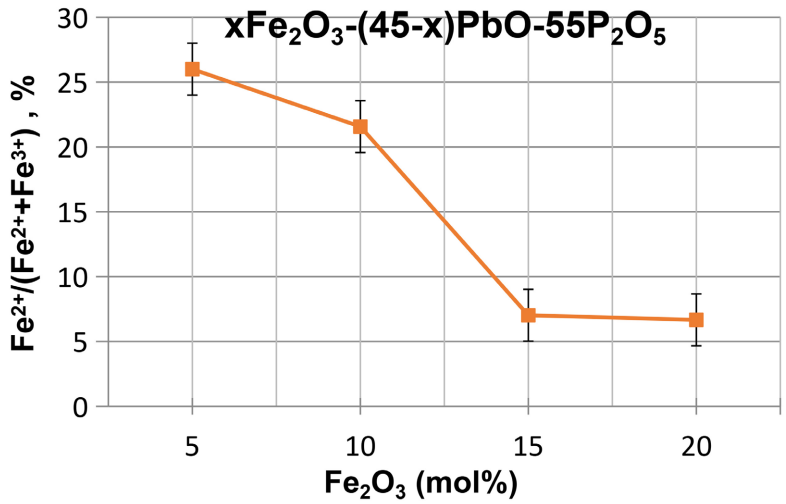

Figure 11. Variation of the $[Fe^{2+}]/[Fe^{2+} + Fe^{3+}]$ ratio versus mol% Fe_2O_3 along the glass series xFe_2O_3-(45-x)PbO-55P_2O_5.

4. Discussions

The glass series xFe_2O_3-(45-x)PbO-$55P_2O_5$ with ($0 \leq x \leq 20$; mol%) were prepared by direct melting at (1050 ± 10)˚C. The structure and the chemical durability of these glasses have been investigated using various techniques such as dissolution rate (D_R), density, IR spectroscopy, X-ray diffraction, SEM and iron redox phenomena. The dissolution rate for all the glasses studied indicates an improvement in chemical durability when the Fe_2O_3 content increases to the detriment of PbO. The variation of transition temperature versus Fe_2O_3 content indicates an increase of T_g from 376˚C to 501˚C when the Fe_2O_3 content increases from 0 to 20 mol%, elucidating an improvement in the rigidity of the glass [19] [20] [29]. The increase both, of the density and the glass transition temperature reflects the strengthening of the Fe-O-P bonds, the electron density becomes very important and leads to a reinforcement of the bonds between the irons and non-bridge oxygen atoms and thus to a reinforcement of the interconnection of the vitreous network chains [11] [28] [30]. The coordination bonds, translated by the hybridization phenomenon, and to the distorted sites occupied by the iron, which become smaller in the phosphate glass compared to the crystalline sites, leads to a reinforcement of the interconnection of the vitreous network chains [28]. The reduction of Fe(III) to Fe(II) in iron-lead-phosphate glasses, is principally due to the presence of ammonium phosphate $(NH_4)_2HPO_4$ in a batch composition as a source of P_2O_5. As a matter of fact, reducing conditions were created during the melting process which favours the reduction of Fe(III) into Fe(II) [1] [17] [28] [29]. Vibrational spectroscopy has allowed us to follow the evolution of the glass structure of iron-lead phosphate glasses. The analyses of the IR spectra revealed that the substitution of Fe_2O_3 at the expense of PbO caused a radical change in phosphate matrix structure. The band observed at 1000 cm^{-1}, when x = 0, can be attributed to the isolated orthophosphate group PO_4^{3-} (Q^0) [21]. When the Fe_2O_3 oxide content increases above 10 mol%, the bands located at 755 cm^{-1} and 1000 cm^{-1} attributed, respectively to the ν_s (P-O-P) and ν_{as} (P-O-P) vibration modes, moves towards high frequencies and indicates the formation of non-bridge oxygen's of pyrophosphate groups (Q^1) to the detriment of the meta-phosphate (Q^2) and orthophosphate (Q^0) groups. The X-ray diffraction spectra confirmed this results, hence, it can be explained that the increase of Fe_2O_3 to the detriment of PbO has the effect of phenomenon seems to play an important role, both, in the viscosity, in the equilibrium between the vitreous bath, in depolymerizing the structure from metaphosphate and/or cyclic metaphosphate and polymerizing isolated orthophosphate chains towards the formation of pyrophosphate chains. This behavior leads to the replacement of the hydrated P-O-P bands and possibly Pb-O-P, by the strongly covalent Fe-O-P bonds. The glass structure can be considered as pyrophosphate units connected with Fe(II) and Fe(III) in octahedral or distorted octahedral coordination [14] [15] [17] [19] [28] [30]. The presence, probably, of Pb(II) and Pb(IV) ions (melting point of PbO_2 is lower than that of PbO) leads to the for-

mation of Pb(IV)-O-P band which is more rigid and covalent than the Pb(II)-O-P band. It contributes to the increase in density and eventually to the formation of pyrophosphates units. Analysis by scanning electron microscope confirmed that the increase in the iron oxide content led to a decrease of crystallites and a polymerization of the structure from the shorter isolated orthophosphate groups towards the majority short pyrophosphate groups which ensures an adequate balance between the crystallites formed and the vitreous bath leading to better chemical durability.

5. Conclusion

The study of glass series xFe_2O_3-(45-x) PbO-$55P_2O_5$, (with $0 \leq x \leq 20$; mol%), indicated a considerable chemical durability. The results obtained confirmed the creation of P-O-M bonds (M = Pb, Fe) with a strongly covalent nature to the detriment of the hydrated P-O-P bonds and led to the formation of majorities pyrophosphate groups. The SEM Micrograph indicated an obvious decrease in crystallites with the increase in Fe_2O_3 content, causing a large equilibrium between the glass bath and the crystallites, hence leading to better chemical durability. The presence, both, of lead in the ion form Pb(II) and Pb(IV) seems to play an important role as well for the viscosity that for the equilibrium between the vitreous bath and the crystalline phases. The dissolution rate (D_R) of the analyzed compounds is 100 times less than to the values of borosilicate glasses and 200 times less than BaBal glass which are used as alternative materials for the immobilisation of nuclear waste substances.

Acknowledgements

The authors wish to thank National Center for Scientific and Technical Research [Division of Technical Support Unit for Scientific Research (TSUSR) Rabat, Morocco] for their assistance to the realization of this work

Conflicts of Interest

The authors declare no conflicts of interest regarding the publication of this paper.

References

[1] Beloued, N., Chabbou, Z. and Aqdim, S. (2016) Correlation between Chemical Durability Behaviour and Structural Approach of the Vitreous Part of the System $55P_2O_5$-$2Cr_2O_3$-(43−x)Na_2O-xPbO. *Advances in Materials Physics and Chemistry*, **6**, 149-156. https://doi.org/10.4236/ampc.2016.66016

[2] Jakhati, S., Nadavalumane, N. and Ashwajeet, J. (2022) Studies of Anomalies in Mixed Conduction of Na_2O and V_2O_5 Doped Boro-Phosphate Glasses. *New Journal of Glass and Ceramics*, **12**, 1-18.

[3] Yu, X., Day, D.E., Long, G.J. and Brow, R.K. (1997) Properties and Structure of Sodium-Iron Phosphate Glasses. *Journal of Non-Crystalline Solids*, **215**, 21-31. https://doi.org/10.1016/S0022-3093(97)00022-7

[4] Kiani, A., Hanna, J.V., King, S.P., Rees, G.J., Smith, M.E., Roohpour, N. and Knowles, J.C. (2012) Structural Characterization and Physical Properties of P_2O_5-CaO-Na_2O-TiO_2 Glasses by Fourier Transform Infrared, Raman and Solid-State Magic Angle Spinning Nuclear Magnetic Resonance Spectroscopies. *Acta Biomaterialia*, **8**, 333-340. https://doi.org/10.1016/j.actbio.2011.08.025

[5] Colak, S.C. and Aral, E. (2011) Optical and Thermal Properties of P_2O_5-Na_2O-CaO-Al_2O_3: CoO Glasses Doped with Transition Metals. *Journal of Alloys and Compounds*, **509**, 4935-4939. https://doi.org/10.1016/j.jallcom.2011.01.172

[6] Videau, J.J. and Gilles, F. (2010) Les verres phosphates de la spécificité de l'atome de phosphore à la formation, la structure et la durabilité chimique de phosphates vitreux. Institut de Chimie de la Matière Condensée de Bordeaux, CNRS, Université de Bordeaux, Bordeaux.

[7] Santic, A., Skoko, Z., Gajovic, A., Reis, S.T., Day, D.E. and Mogus-Milankovic, A. (2011) Physical Properties of Lead Iron Phosphate Glasses Containing Cr_2O_3. *Journal of Non-Crystalline Solids*, **357**, 3578-3584. https://doi.org/10.1016/j.jnoncrysol.2011.07.011

[8] Makhkhas, Y., Aqdim, S. and Sayouty, E.H. (2013) Study of Sodium-Chromium-Iron-Phosphate Glass by XRD, IR, Chemical Durability and SEM. *Journal of Materials Science and Chemical Engineering*, **1**, 1-6. https://doi.org/10.4236/msce.2013.13001

[9] Aqdim, S., Errouissi, Y., Cherif, A. and Makhlouk, R. (2017) Elaboration and Characterization of Glasses and Ceramic-Glasses within the Ternary Diagram Li_2O-Cr_2O_3-P_2O_5. *Advances in Materials Physics and Chemistry*, **7**, 123-137. https://doi.org/10.4236/ampc.2017.74011

[10] El-Egili, K., Doweidar, H., Moustafa, Y.M. and Abbas, I. (2008) Structure and Some Properties of PbO-P_2O_5 Glasses. *Physica B*, **339**, 237-245. https://doi.org/10.1016/j.physb.2003.07.005

[11] Brow, R.K. (2000) Review: The Structure of Simple Phosphate Glasses. *Journal of Non-Crystalline Solids*, **263-264**, 1-28. https://doi.org/10.1016/S0022-3093(99)00620-1

[12] Er-Rouissi, Y., *et al.* (2020) Chemical Durability, Structure Properties and Bioactivity of Glasses $48P_2O_5$-30CaO-(22−x)Na_2O-xTiO_2 (With $0< x \leq 3$; mol%). *Advances in Materials Physics and Chemistry*, **10**, 305-318. https://doi.org/10.4236/ampc.2020.1012024

[13] Errouissi, Y., Chabbou, Z., Beloued, N., Aqdim, S. and Aqdim, S. (2017) Chemical Durability and Structural Properties of Al_2O_3-CaO-Na_2O-P_2O_5 Glasses Studied by IR Spectroscopy, XRD and SEM. *Advances in Materials Physics and Chemistry*, **7**, 353-363. https://doi.org/10.4236/ampc.2017.710028

[14] Aqdim, S. (2007) Investigation des phases vitreuses des systèmes $(Li, Na)_2O$-$(Fe, Al)_2O_3$-P_2O_5 par Spectroscopies Infrarouge et Mössbauer-Structures et Durabilité chimique. These, Faculté des Sciences de Casablanca Ain Chock, Casablanca.

[15] Aqdim, S., Elouadi, B. and Grenech, J.M. (2012) Chemical Durability and Structural Approach of the Glass Series (40−y)Na_2O-yFe_2O_3-5Al_2O_3-55$P_2O_5$by IR, X-Ray Diffraction and Mössbauer Spectroscopy. *Material Sciences and Engineering*, **27**, Article ID: 012003. https://doi.org/10.1088/1757-899X/28/1/012003

[16] Chabbou, Z. and Aqdim, S. (2014) Chemical Durability and Structural Proprieties of the Vitreous Part of the System xCaO-(40−x)ZnO-15Na_2O-45P_2O_5. *Advances in Materials Physics and Chemistry*, **4**, 179-180. https://doi.org/10.4236/ampc.2014.410021

[17] Ouchetto, M. (1993) Thèse de Doctorat d'Etat es Sciences. Faculty of Sciences Rabat, Rabat.

[18] Aqdim, S. and Albizane, A. (2015) Structural Feature and Chemical Durability of Sodium Aluminium Iron Phosphate Glasses. *Journal of Environmental Science, Computer Science and Engineering & Technology*, **4**, 509-521.

[19] Santic, A., Mogus-Milankovic, A., Furic, K., Bermanec, V., Kim, D.W. and Daye, D.E. (2007) Structural Properties of Cr_2O_3-Fe_2O_3-P_2O_5 Glasses, Part I. *Journal of Non-Crystalline Solids*, **353**, 1070-1077. https://doi.org/10.1016/j.jnoncrysol.2006.12.104

[20] Ingram, M.D., Imre, C.T. and Konidakis, I. (2006) Activation Volumes and Site Relaxation in Mixed Alkali Glasses. *Journal of Non-Crystalline Solids*, **352**, 3200-3209. https://doi.org/10.1016/j.jnoncrysol.2006.05.009

[21] Imre, A., Divinski, S.V., Voss, S., Berkmeier, F. and Mehrer, H. (2006) A Revised View on the Mixed-Alkali Effect in Alkali Borate Glasses. *Journal of Non-Crystalline Solids*, **352**, 783-788. https://doi.org/10.1016/j.jnoncrysol.2006.02.008

[22] Aqdim, S., Sayouty, E.H. and Elouadi, B. (2008) Structural and Durability Investigation of the Vitreous Part of the System $(35-z)Na_2O$-zFe_2O_3-$5Al_2O_3$-$60P_2O_5$. *Eurasian Chemico-Technological Journal*, **10**, 9-17.

[23] Bevilacqua, A.M., *et al.* (1996) Immobilization of Simulated High-Level Liquid Wastes in Sintered Borosilicate, Aluminosilicate and Aluminoborosilicate Glasses. *Journal of Nuclear Materials*, **229**, 187-193. https://doi.org/10.1016/0022-3115(95)00229-4

[24] Aqdim, S. and Ouchetto, M. (2013) Elaboration and Structural Investigation of Iron (III) Phosphate Glasses. *Advances in Materials Physics and Chemistry*, **3**, 332-339. https://doi.org/10.4236/ampc.2013.38046

[25] Mogus-Milankovic, A., Santic, A., Reis, S.T., Furic, F. and Day, D.E. (2005) Studies of Lead-Iron Phosphate Glasses by Raman, Mössbauer and Impedance Spectroscopy. *Journal of Non-Crystalline Solids*, **351**, 3246-3258. https://doi.org/10.1016/j.jnoncrysol.2005.08.006

[26] Bachachir, B., Er-Rouissi, Y., Makhlouk, R., Harrati, H., El Bouari, A. and Aqdim, S. (2021) Structural Features and Properties of the Vitreous Part of the System $50P_2O_5$-$25CaO$-$(25-x)Na_2O$-$xCoO$ (with $0 \le x \le 25$; mol%). *Advances in Materials Physics and Chemistry*, **11**, 254-266. https://doi.org/10.4236/ampc.2021.1112021

[27] Doweidar, H., Moustafa, Y.M., El-Egili, K. and Abbas, I. (2005) Infrared Spectra of Fe_2O_3-PbO-P_2O_5 Glasses. *Vibrational Spectroscopy*, **37**, 91-96. https://doi.org/10.1016/j.vibspec.2004.07.002

[28] Reis, S.T., Karabulut, M. and Day, D.E. (2001) Chemical Durability and Structure of Zinc-Iron Phosphate Glasses. *Journal of Non-Crystalline Solids*, **292**, 150-157. https://doi.org/10.1016/S0022-3093(01)00880-8

[29] Srinivasa Reddy, M., Naga Raju, G., Nagarjuna, G. and Veeraiah, N. (2007) Structural Influence of Aluminium, Gallium and Indium Metal Oxides by Means of Dielectric and Spectroscopic Properties of CaO-Sb_2O_3-B_2O_3 Glass System. *Journal of Alloys and Compounds*, **438**, 41-51. https://doi.org/10.1016/j.jallcom.2006.08.054

[30] Beloued, N., Makhlouk, R., Er-Rouissi, Y., Taibi, M., Sajieddine, M. and Aqdim, S. (2019) Relationship between Chemical Durability, Structure and the Ionic-Covalent Character of Me-O-P Bond (Me = Cr, Fe), in the Vitreous Part of the System $60P_2O_5$-$2Cr_2O_3$-$(38-x)Na_2O$-xFe_2O_3 (with $3 \le x \le 33$ mol%). *Advances in Materials Physics and Chemistry*, **9**, 199-209.